


## RESEARCH ARTICLE

# Personalized Surgical Planning for Soft Tissue Sarcoma of the Popliteal Fossa with a Novel 3D Imaging Technique

Xiang Fang, MD, PhD<sup>1</sup>, Fang Yuan, MD, PhD<sup>2</sup>, Yan Xiong, MD, PhD<sup>1</sup>, Senlin Lei, MD, PhD<sup>1</sup>, Dechao Yuan, MD, PhD<sup>1</sup>, Yong Zhou, MD, PhD<sup>1</sup>, Wenli Zhang, MD, PhD<sup>1</sup>, Chongqi Tu, MD<sup>1</sup>, Hong Duan, MD, PhD<sup>1</sup> 

Department of <sup>1</sup>Orthopedics, Orthopedic Research Institute, West China Hospital and <sup>2</sup>Radiology, West China Hospital, Sichuan University, Chengdu, People's Republic of China

**Objective:** Soft tissue sarcomas (STSs) arising from the popliteal fossa pose surgical challenges due to their proximity to critical neurovascular structures. This study aimed to investigate whether a novel 3D imaging technique highlighting these key anatomical structures could facilitate preoperative planning and improve surgical outcomes in STS.

**Methods:** This was a prospective, observational, pilot study. Between November 2019 and December 2020, 27 patients with STS of the popliteal fossa undergoing limb-sparing procedures were enrolled and assigned to either a control or intervention group. Control patients underwent traditional preoperative planning with separate computed tomography angiography, magnetic resonance imaging, and magnetic resonance hydrography. In the intervention group, 3D images were generated from these images, the tumor and skeletomuscular and neurovascular structures were revealed in three dimensions, and this was visualized on the surgeon's smartphone or computer. Primary endpoints were surgical margins and complications. Secondary endpoints included operative time, blood loss, serum C-reactive protein and interleukin-6, length of in-hospital stay, and limb function. Comparisons between groups were made using independent-sample t-tests for continuous data and the Mann–Whitney U and Fisher's exact tests for categorical data.

**Results:** There was a lower but not significantly different inadvertent positive margin rate (1/15 vs. 3/12,  $P = 0.294$ ), significantly shorter hospital stay ( $P = 0.049$ ), and less numbers  $\geq 75$ th percentile of operative time ( $P = 0.037$ ) and blood loss ( $P = 0.024$ ) in the intervention group. Differences in surgical complications, operative time, blood loss, C-reactive protein and interleukin-6 levels on the second postoperative day, and limb functional scores were statistically insignificant.

**Conclusions:** The novel 3D imaging technique facilitates complex preoperative planning and limb-salvage surgical procedures for patients with STS of the popliteal fossa, and this may affect how surgical planning is performed in the future.

**Key words:** 3D imaging; Length of hospital stay; Neurovascular evaluation; Personalized surgery; Popliteal fossa

## Introduction

Soft tissue sarcomas (STSs) account for approximately 1% of all malignancies in adults and have more than a hundred subtypes.<sup>1–4</sup> An estimated 13,460 new STS diagnoses

were made in the U.S. in 2021, along with 5350 related deaths.<sup>5</sup> The common histotypes include liposarcoma, leiomyosarcoma, and undifferentiated pleomorphic sarcoma, with the most typical primary sites being the extremities

**Address for correspondence** Hong Duan, MD, PhD and Wenli Zhang, MD, PhD, Department of Orthopedics, Orthopedic Research Institute, West China Hospital, Sichuan University, 37 Guo Xue Lane, Chengdu, Sichuan 610064, People's Republic of China.

Email: [duanhong1970@126.com](mailto:duanhong1970@126.com) and [zwlbox@163.com](mailto:zwlbox@163.com)

Xiang Fang and Fang Yuan contributed equally to this work, and they are first co-authors.

Received 28 June 2022; accepted 21 August 2022

(40%–50%), trunk (13%), and retroperitoneal space (7%).<sup>1,6,7</sup> Despite considerable progress in transdisciplinary management, surgery remains the mainstay of curative treatment, with *en bloc* resection and wide surgical margins being the standard approach.<sup>8,9</sup>

Accounting for less than 5% of all extremity and trunk STSs, the popliteal fossa is a relatively rare anatomic site of involvement that poses special management challenges due to the proximity of crucial neurovascular bundles.<sup>10–12</sup> Wide surgical margins become almost impossible in such conditions, and functional morbidity increases.<sup>13</sup> Further radiation treatment, either prior to or following surgical resection, can be employed for local control; however, potential complications include neuritis, joint stiffness, edema, fibrosis, pain, and wound issues.<sup>14,15</sup> Surgical margin contamination may be minimized with appropriate surgical planning by experienced surgeons, thereby requiring fewer total radiation doses, resulting in better limb function and greater local control. Additionally, this process may also limit accidental intraoperative injury to major neurovascular structures. Nevertheless, only a few studies have reported clinical improvement based on the use of preoperative images, which form the basis of surgical planning.<sup>16–18</sup> MRI and magnetic resonance hydrography are the principal tools for surgical planning, particularly for assessing tumor spatial location and its relationship to adjacent nerves, generally in two dimensions (2D). CT identifies vascular structures and calcifications in 3D. The traditional preoperative planning process requires the surgeon to construct the tumor and surrounding critical anatomical structures by screening and synthesizing necessary information from individual 2D and 3D images, a highly cognitively demanding process that requires expertise but, most importantly, could be subjective or even inaccurate.

Therefore, a novel 3D image tumor model is generated by registering and segmenting multimodal images synergistically to give more comprehensive guidance for diagnosis and treatment. Although surgeons are trained to recognize and mentally integrate various key anatomical structures from multiple images, the digital fusion display of multimodal images could provide additional information and be more diagnostically accurate than conventional mental representations.<sup>19</sup> While the novel 3D imaging technique has been successfully applied in neurosurgery, radiation therapy, and bone oncology surgery,<sup>20–23</sup> no relevant studies have been published on its use in STS of the popliteal fossa. The purpose of this study was to: (i) compare the early surgical outcome based on the novel 3D image vs traditional images for patients with STS of the popliteal fossa; and (ii) state advantages of the use of the novel 3D imaging technique for the personalized surgical treatment of STS.

## Materials and Methods

### Study Design

This was a prospective, observational, pilot study comparing surgical planning and outcomes based on the novel 3D image vs traditional images in the context of STS of the

popliteal fossa (ChiCTR.org, ChiCTR2000041043). The ethical committee of our hospital approved the study protocol (No. 2019–1062). The Strengthening the Reporting of Observational Studies in Epidemiology (STROBE) reporting guidelines were followed (Fig. 1).

### Subjects and Management

The eligibility requirements were STS of the popliteal fossa (diameter >5 cm), which was biopsy-proven, resectable, and treatment-naïve; age >14 years; and aiming for curative limb-salvage surgery. Patients with severe systemic disease and intolerance to surgery were excluded. Written informed consent was obtained from patients or guardians.

The patients were allocated to either the intervention (with novel 3D image) or the control (with traditional images) group, based on their preference. Each case was reviewed by a transdisciplinary team composed of pathologists, radiologists, orthopedic surgeons, radiation specialists, and medical oncologists. Preoperative chemotherapy was indicated as per the pathological diagnosis from biopsy, whereas preoperative radiation treatment was performed

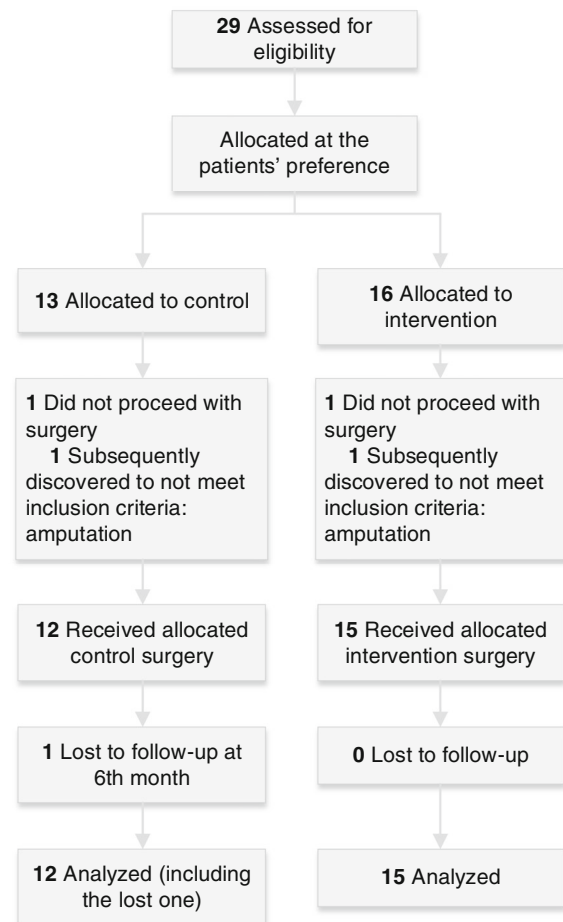


Fig. 1 Flow chart of participant inclusion in this study

when obtaining an oncologically appropriate surgical margin was difficult.<sup>24</sup>

Preoperative local imaging included contrast-enhanced CT angiography, contrast-enhanced MRI, and magnetic resonance hydrography for both groups. A surgeon (H.D. or C.T.) with >15 years of experience in STS conducted the surgical planning and the curative surgery. The surgical plan for the intervention group was based on the novel 3D image, while for the control group, it was carried out using traditional classic images.

Similar intraoperative and postoperative treatments were followed for both groups. The dissection was performed through grossly normal planes of tissue without tumor involvement. Where the tumor had adhered to bone, the periosteum was excised. In cases of cortical or medullary involvement, the segment was removed and reconstructed. Tumors adjacent to major vessels were not removed when the underlying structures were in grossly intact condition following adventitia resection. Otherwise, the vessels were resected, followed by bypass graft surgery. The major nerves

were always preserved, with the perineurium removed when immediately adjacent to the tumor.

Postoperative radiation treatment was considered for cases with positive margins, and those with stage II, IIIA, and IIIB disease, as per the American Joint Committee on Cancer (AJCC) *Staging system for soft tissue sarcoma of the trunk and extremities* (8th ed., 2017).<sup>1,24,25</sup> Chemotherapy was also recommended for specific subtypes. Patients were followed up at 2 weeks, 1 month, 3 months, and 6 months after surgery, and every 3–6 months thereafter at outpatient clinics, where chest CT and localized MRI scans were taken (except at 2 weeks).

### 3D Image Preparation

The intervention group utilized Digital Imaging and Communications in Medicine (DICOM) data from CT, MRI, and magnetic resonance hydrography were used to construct the tumor model in 3D, based on the report by Fang et al.<sup>21</sup> The voxel size for CT angiography image and magnetic resonance hydrography image was 0.8 mm × 0.8 mm × 0.8 mm and

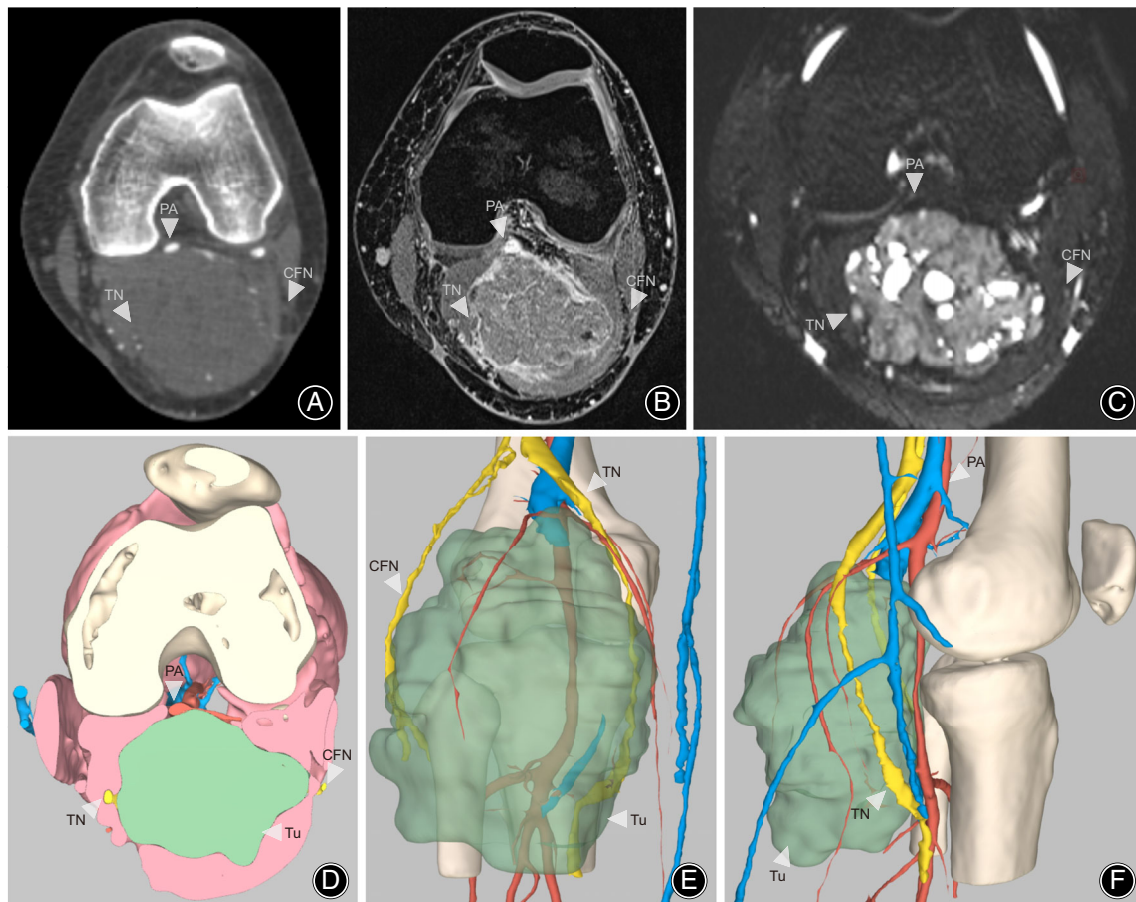


**Fig. 2** Classic images and three-dimensional reconstruction in a patient with popliteal fossa synovial sarcoma. CT angiography image (A), T1-weighted MRI (B), MR hydrography image (C), 3D reconstruction image (D) in similar axial views. Posterior and lateral view of the 3D reconstruction image (E, F). Abbreviations: PA, popliteal artery; CFN, common fibular nerve; TN, tibial nerve; Tu, tumor

0.4 mm × 0.4 mm × 1.0 mm (axial spacing × sagittal spacing × coronal spacing), respectively, whereas the voxel size for other images varied with a slice thickness between 3 and 5 mm. The MR images were mapped to CT images with affine and diffeomorphic registration algorithms using advanced normalization tools (<https://github.com/ANTsX/ANTs>). To segment the tumor and its surrounding vital anatomical structures, several semi-automatic segmentation algorithms were employed, such as level-set, region-grow, and threshold control, in the interactive software 3D Slicer 4.11 (3D Slicer, [www.slicer.org](http://www.slicer.org)).<sup>26</sup> Quality assurance and artificial correction processes were conducted to ensure a registration accuracy of >95% and a maximum segmentation error of <2 mm, referring to the original raw DICOM data. The time spent for 3D reconstruction was recorded.

The 3D image model included the bone, sarcoma, major neurovascular bundles (in proximity to the sarcoma), muscles, enlarged lymph nodes (if any), and bone edema (if any) and were viewed by surgeons *via* mobile applications or computers (Fig. 2). The application used was 3D PDF Reader 3.4 (Tech Soft 3D, Bend, OR, USA). With standard smartphone gestures and simple configurations, the patient-specific 3D model, or any part of it, can be rotated, zoomed, hidden, displayed, and rendered translucent.

### Outcome Measures

The enrollment period was from November 2019 to December 2020, and the data were collected between November 2019 and June 2021. Recorded baseline characteristics included sex, age, tumor size, pathological diagnosis, Fédération Nationale des Centres de Lutte Contre le Cancer (FNCLCC) tumor grading, stage, and presence of neurovascular involvement.<sup>27</sup> Tumor size was determined from preoperative cross-sectional images by measuring the maximum diameter of the tumor on MRI. Neurovascular involvement was defined as >50% complete envelope in preoperative images that presented difficulty in anatomical dissection.

The primary outcome measures were the surgical margins and complications. The surgical margins were first recorded intraoperatively and later confirmed by pathological analysis using the Toronto Margin Context Classification (TMCC).<sup>28</sup> The margins were classified into four types: negative, the same as AJCC's R0; inadvertent positive margins (IPMs); planned close with an ultimately positive microscopic margin along a major bone or neurovascular structure; and whoops margin, positive after a second resection for patients treated initially elsewhere with inadequate margins. Accidental injury to vessels and nerves and issues with wound healing were key complications of interest. Vascular injury was

**TABLE 1 Patient baseline characteristics**

Characteristic	Participants, No. (%)		Statistic Value	P Value
	Control (n = 12)	3DMMI (n = 15)		
Age, mean (SD), years	42.8 (13.5)	39.5 (16.5)	t = 0.5556	0.583 <sup>d</sup>
Sex			$\chi^2 = 0.0675$	>0.999 <sup>e</sup>
Male	7 (58)	8 (53)		
Female	5 (42)	7 (47)		
Histological type			$\chi^2 = 1.9675$	0.854 <sup>e</sup>
Synovial sarcoma	4 (33)	3 (20)		
Undifferentiated pleomorphic sarcoma	1 (8)	4 (27)		
Liposarcoma	3 (25)	3 (20)		
Well-differentiated liposarcoma	1 (8)	0		
Dedifferentiated liposarcoma	1 (8)	2 (13)		
Myxoid liposarcoma	1 (8)	1 (7)		
Rhabdomyosarcoma	2 (17)	2 (13)		
Myxofibrosarcoma	1 (8)	2 (13)		
Angiosarcoma	1 (8)	1 (7)		
FNCLCC grade			U = 82.5	0.667 <sup>f</sup>
1	1 (8)	1 (7)		
2	4 (33)	4 (27)		
3	7 (58)	10 (67)		
Tumor Size <sup>a</sup> , mean (SD), cm	11.2 (3.0)	11.3 (3.5)	t = 0.9183	0.367 <sup>d</sup>
Neurovascular involvement				
Vessel	5 <sup>b</sup> (42)	5 <sup>c</sup> (33)	$\chi^2 = 0.1985$	>0.706 <sup>e</sup>
Nerve	6 <sup>b</sup> (58)	8 <sup>c</sup> (67)	$\chi^2 = 0.0297$	>0.999 <sup>e</sup>
Tumor Stage			U = 79.5	0.567 <sup>f</sup>
IB	1 (8)	1 (7)		
IIIA	6 (50)	6 (40)		
IIIB	5 (42)	8 (53)		

Notes: <sup>a</sup>Tumor size was recorded in maximum diameter.; <sup>b</sup>Four patients had both vessel and neural involvement.; <sup>c</sup>Four patients had both vessel and neural involvement.; <sup>d</sup>Student's T-test.; <sup>e</sup>Fisher exact test for major types of histology, not considering the subtypes of liposarcomas.; <sup>f</sup>Wilcoxon rank sum test. Control group patients underwent preoperative planning with traditional classic images, and intervention group with the novel 3D image.



**TABLE 2 Surgical outcomes for curative surgery of the soft tissue sarcomas of the popliteal fossa**

Outcome	Control (n = 12)	3DMMI (n = 15)	Statistic Value	P Value
Surgical margin, No. (%)			U = 81.5	0.651 <sup>a</sup>
Negative	5 (42)	6 (40)		
Planned close	4 (33)	8 (53)		
IPM	3 (25)	1 (6)	$\chi^2 = 1.7755$	0.294 <sup>b</sup>
Surgical complications, No. (%)	3 (25)	1 (6)	$\chi^2 = 1.7755$	0.294 <sup>b</sup>
Intraoperative, vascular injury	1 (8)	0	$\chi^2 = 1.2981$	0.444 <sup>b</sup>
Intraoperative, nerves injury	2 (17)	1 (6)	$\chi^2 = 0.6750$	0.569 <sup>b</sup>
Postoperative, wound complication	0	0		
Operative time, mean (SD), min				
Mean (SD)	106.7 (26.05)	87.33 (25.20)	t = 1.9510	0.062 <sup>c</sup>
Median (IQR)	120 (37.5)	80 (30.0)		
≥75th Percentile, participants, No. (%) <sup>d</sup>	7 (58)	2 (13)	$\chi^2 = 6.0750$	0.037 <sup>b</sup>
Blood loss (ml)				
Mean (SD)	199.2 (113.4)	148.7 (59.51)		
Median (IQR)	225 (215)	150 (30)	U = 71.5	0.375 <sup>a</sup>
≥75th Percentile, participants, No. (%) <sup>d</sup>	6 (50)	1(7)	$\chi^2 = 6.5186$	0.024 <sup>b</sup>
Serum index of systemic inflammation				
CRP, preoperative, median (IQR), mg/L	4.09 (1.33)	3.81 (0.74)	U = 86.0	0.867 <sup>a</sup>
IL-6, preoperative, median (IQR), pg./mL	2.86 (1.36)	3.17 (1.22)	U = 86.5	0.876 <sup>a</sup>
CRP, at 2nd day, mean (SD), mg/L	37.61 (10.10)	34.92 (5.80)	t = 0.8690	0.393 <sup>c</sup>
IL-6, at 2nd day, mean (SD), pg./mL	32.13 (7.65)	28.93 (5.89)	t = 1.2310	0.230 <sup>c</sup>
Length of in-hospital stay, median (IQR)	8(1.75)	7(2.00)	U = 50.5	0.049 <sup>a</sup>
Limb Function				
MSTS, preoperative, median (IQR)	93 (5.3)	93 (6.0)	U = 86.5	0.874 <sup>a</sup>
MSTS, at 6th month, median (IQR)	93 (8.3)	93 (7.0)	U = 81.0	0.666 <sup>a</sup>

Notes: Control group patients underwent preoperative planning with traditional classic images, and intervention group with the novel 3D image.; Abbreviations: CRP, C-reactive protein; IL-6, interleukin-6; IPM, inadvertent positive margins.; <sup>a</sup>Wilcoxon rank sum test.; <sup>b</sup>Fisher exact test.; <sup>c</sup>Student's *T*-test.; <sup>d</sup>75th percentiles are defined as 120 min for operative time and 250 mL for blood loss.

defined as inadvertent injury where suture repair was needed. Nerve injury was defined as an injury associated with limb malfunction after surgery.

The secondary outcome measures were operative time, estimated intraoperative blood loss, serum index of systemic inflammation C-reactive protein (CRP) and interleukin-6 (IL-6), length of in-hospital stay, and Musculoskeletal Tumor Society (MSTS) limb function score.<sup>29</sup> The operative time and estimated intraoperative blood loss amount were also classified as <75th and ≥75th percentiles, which were chosen as an indicator of surgical quality. CRP and IL-6 were chosen to reflect the magnitude of the systemic inflammatory response associated with operative trauma and were assessed preoperatively and at 2 days postoperatively.<sup>30,31</sup> The MSTS was evaluated preoperatively and at 6 months following surgery. Other information on survival, including evidence of local recurrence and metastasis, was also recorded.

### Statistical Analysis

Sample size estimation was not undertaken due to the lack of previously published data. The Shapiro–Wilk test was used to examine if continuous variables were normally distributed. For normal distributions, the mean was calculated (with standard deviation [SD]); otherwise, median values were reported (with interquartile range [IQR], or range). Categorical data are expressed as proportions (percentages).

Comparisons between groups were made using independent-sample *t*-tests for continuous data and the Mann–Whitney *U* and Fisher's exact tests for categorical data. Analyses were conducted using R 3.5.3 (R Foundation for Statistical Computing, Vienna, Austria), and a two-sided *P* value of <0.05 was considered statistically significant.

## Results

### Baseline Characteristics

Between November 2019 and December 2020, 29 patients with STS of the popliteal fossa were identified, of whom two were excluded for requiring amputations following admission. A total of 27 patients were included, of whom 15 were males, with a mean age of 40.9 [15.1] years. Twelve patients were assigned to the control group and 15 to the intervention group based on their personal preferences. No statistical differences in patient baseline characteristics were found between the two groups (Table 1).

### Primary Outcomes

The overall surgical margins (*P* = 0.671), IPM (1/15 vs. 3/12, *P* = 0.294), and intraoperative complications (*P* = 0.294) were not statistically significant.

### Secondary Outcomes

The secondary outcome differences between the two groups were not statistically significant in terms of the operative time ( $P = 0.062$ ), and estimated intraoperative blood loss ( $P = 0.375$ ), nor were the differences significant for the 2nd-day serum CRP ( $P = 0.383$ ) and IL-6 ( $P = 0.230$ ) levels postoperatively, and MSTs ( $P = 0.666$ ) at the 6th month. Significant differences were found in length of stay ( $P = 0.049$ ), numbers  $\geq 75$ th percentile vs  $< 75$ th percentile of operative time ( $P = 0.037$ ), and blood loss ( $P = 0.024$ ) (Table 2). One patient in each group required vascular bypass graft surgery due to gross tumor involvement.

### Miscellany

The time spent on 3D reconstruction was 3–4 h (median, 3.5h) per patient. The median follow-up duration was 12 months (range, 6–18 months). One patient from the control group was lost to follow-up 6 months postoperatively. At the last follow-up at 18 months, one patient from the intervention group had lung metastasis without local recurrence. All other patients had been disease free. The MSTs (preoperatively vs 6 months after surgery) were not statistically significant for the control ( $P = 0.656$ ) and intervention ( $P = 0.125$ ) groups.

### Discussion

STSs of the popliteal fossa with proximity to vital neurovascular bundles and occasional involvement were a challenge for the surgeons.<sup>32</sup> Tumor location, especially spatial distance to major neurovascular structures, is essential for surgical planning and outcome prognosis.<sup>10</sup> However, literature focusing specifically on ways to improve surgical outcomes from the perspective of surgical planning based on 3D imaging that reveal these critical anatomical structures is very limited. Here, we showed that the novel 3D imaging technique contributed to improved surgical planning for patients with STS of the popliteal fossa, resulting in shorter hospital stays, less numbers of high blood loss and long operative time, and a potentially lower risk of IPM. Surgeons are, therefore, recommended to use multimodal images for 3D reconstruction when treating complicated STSs, particularly those with neurovascular involvement.

### Personalized Surgical Planning

A comprehensive knowledge of anatomy is essential for a successful surgery. While some experienced surgical oncologists can accomplish any limb-salvage STS surgery despite any unexpected intraoperative findings of innate or tumor-related anatomical variations, young surgeons are at a greater risk of injuring major neurovascular structures or of prolonging surgical duration, especially in patients with difficult anatomy. Hence, surgical planning based on images is necessary. During the traditional classic procedure, surgeons need to identify every key anatomical structure to form a roughly patient-specific tumor model in their brain preoperatively. Although radiologists are usually more capable of

reading medical images, their knowledge of patient-specific anatomy cannot be fully utilized by surgeons. Nevertheless, during the improved surgical planning, the novel 3D image was processed by an experienced radiologist. This 3D model was an excellent tool to connect the surgeons and radiologists, thereby facilitating better multidisciplinary teamwork. By this intuitive and informative computer-generated 3D representation, all detailed patient-specific knowledge can be translated into real surgical benefits against all potential intraoperative anatomical challenges. Based on the digital 3D model revealing the tumor and all adjacent key anatomical structures, a tailored individualized preoperative plan can be easily devised that can hardly be accomplished with traditional separate images, or in a very rough fashion. This included *via* which muscle or compartment the resection should be performed, whether to remove a major vessel or its adventitia only, the suitable site and length of resection, if necessary, and from which plane the dissection should be performed for a major neurovascular structure in proximity to the tumor. This evaluation is possible even when these structures are pushed aside, far from the original standard anatomical location, by the tumor. This situation can be difficult, even for some STS experts but particularly so for less experienced surgeons. In most cases, the surgical plan is formulated after the tumor surroundings are visualized intraoperatively. Hence, by using the novel 3D image, the risk of accidental invasion of the tumor and major neurovascular injury can be minimized and operating time reduced, especially in complex cases for less experienced surgeons.

### Resection Margin

This study used the TMCC to evaluate the resection margin rather than the AJCC residual tumor classification or the Enneking systems because TMCC has unique applications in the context of inadvertent residuals (IPMs).<sup>28</sup> However, there were nearly a quarter as many IPMs in the intervention group as in the control group (1/15 vs 3/12), with no statistical difference, which was attributed to the relatively small sample size. Nonetheless, this pilot study examined early clinical outcomes and reported an institution's preliminary experience, suggesting rationality for future large-scale trials.

### Surgical Metrics

To achieve a successful limb-salvage STS operation, surgical metrics, including surgical complications, operative time, blood loss, serum index of systemic inflammation, limb function, and length of in-hospital stay, are crucial. In this study, total operative time, total blood loss, intraoperative complications, inflammation index, and limb function were similar between the two groups. However, the number of cases with  $\geq 120$  min (75th percentile) of operative time and  $\geq 250$  mL (75th percentile) blood loss, were significantly reduced in the intervention group. This suggested that the novel 3D image may assist surgeons predominantly in complex cases by facilitating preoperative decision-making and minimizing

surgical challenges related to uncertain or inconspicuous anatomical parameters. Furthermore, the length of in-hospital stay was significantly shorter in the intervention group. This may decrease the risk of in-hospital complications, saving costs and healthcare resources.<sup>33</sup> Therefore, surgical planning based on the novel 3D image is a promising strategy for achieving successful limb-salvage STS procedure.

### Benefits for Surgeons

Besides the previously mentioned merits for patients and hospitals, surgical planning based on the novel 3D image also helps surgeons alleviate the cognitive burden exerted on surgeons by decreasing the magnitude of information that needs to be processed.<sup>34</sup> Conventional raw images, such as CT and MRI, display all aspects of anatomical information in grayscale, where structures unrelated to surgical decision-making are also included. Such extraneous information may impair surgeons' cognition and affect their judgment when interpreting imaging. However, irrelevant information was excluded in the 3D image, and only key structures and their spatial relationships were highlighted more understandably in a multicolor format in 3D, allowing easier preoperative planning.

### Caution before Further Application

Despite advantages shown in surgical planning, the shift of anatomical structures related to the patient position between preoperative imaging and surgery should not be neglected, which may lead to inaccurate representation of the 3D image. The mean shift of the sciatic nerve (in the upper leg) and tibial nerve (in the lower leg) for repeated supine positions is 3.06 mm and 0.9 mm, respectively, and 5.86 mm and 3.02 mm for supine vs. other patient positions, respectively.<sup>18</sup> Accordingly, patient position during imaging acquisition should be consistent with that employed in the operation room to minimize the variability, particularly for 3D reconstruction for sarcomas in less rigid regions.

### Strengths and Limitations

To our knowledge, this is the first prospective study that explored the use of the novel 3D imaging technique for the personalized surgical treatment of STS in the popliteal fossa. Nevertheless, our study had several limitations. First, the sample size was small, limiting statistical analyses. The limited availability of data from the literature also prevented us from calculating the sample size. However, this was intended as a pilot study to explore a novel preoperative planning tool for rare tumors in challenging locations, which could serve as the basis for future large-scale trials. Second, the follow-up

period was short. However, this study aimed to describe intraoperative conditions and early surgical outcomes associated with preoperative planning instead of long-term survival or metastasis. Third, two patients were excluded from our analysis, which may have affected the overall results. Fourth, the fact that the operation in this research was performed by experienced surgeons with over 15 years of experience may understate the validity and strength for this novel 3D image among less experienced surgeons.

### Conclusions

In this real-world pilot study, we found that the preoperative planning for cases with complex STS of the popliteal fossa was improved through the novel 3D image, as it enhanced surgical planning procedures with a positive impact on the patients, surgeons, and hospital. Patients could experience decreased intraoperative blood loss, shorter operating times, and potentially reduced risks of inadvertent residuals. For surgeons, using the novel 3D image may also provide an intuitive and comprehensive approach to comprehensive patient-specific knowledge of anatomy and tailored personalized surgical planning, while hospitals would benefit from reduced costs and resources associated with improved patient outcomes. Overall, this study yielded promising results with this novel 3D imaging technique that could guide future studies and advance preoperative planning.

### Acknowledgments

This work was funded by West China Hospital Sichuan University Science Funds (NO. 141120752), and Health and Family Planning Commission research project of Sichuan Province (NO. 18PJ465). No benefits in any form have been or will be received from a commercial party directly or indirectly related to the subject of this manuscript. Special thanks to Jianqing Qiu from the Department of Epidemiology and Health Statistics, West China School of Public Health, Sichuan University, China, for the statistical assistance in this study.

### Author Contributions

All authors had full access to the data in the study and take responsibility for the integrity of the data and the accuracy of the data analysis. *Conceptualization*, X.F., Y.X., F.Y., W.Z. and H.D.; *Data curation*, X.F., S.L., D.Y., Y.Z., W.Z., C.T. and H.D.; *Funding acquisition*, H.D., Y.X.; *Methodology*, X.F., Y.X. and F.Y.; *Resources*, S.L., D.Y., Y.Z., W.Z., C.T. and H.D.; *Supervision*, W.Z. and H.D.; *Writing – original draft*, X.F., Y.X. and F.Y.; *Writing – review & editing*, X.F., Y.X., F.Y., S.L., D.Y., Y.Z., W.Z., C.T. and H.D.

### References

- Gamboia AC, Gronchi A, Cardona K. Soft-tissue sarcoma in adults: an update on the current state of histiotype-specific management in an era of personalized medicine. *CA Cancer J Clin.* 2020;70(3):200–29.
- Wang B, Chen LJ, Wang XY. A clinical model of bone angiosarcoma patients: a population-based analysis of epidemiology, prognosis, and treatment. *Orthop Surg.* 2020;12(6):1652–62.
- Qiao J, Mao H, Wen L, Xu L, Zhu Z, Qiu Y, et al. Reconstruction of soft tissue defect with a free vascularized anterolateral thigh flap after resection of soft tissue sarcoma in extremities. *Orthop Surg.* 2022;14(2):215–20.
- Choi JH, Ro JY. The 2020 WHO classification of tumors of soft tissue: selected changes and new entities. *Adv Anat Pathol.* 2021;28(1):44–58.

5. Bickels J, Malawer MM. Adult soft-tissue sarcomas of the extremities. *J Bone Joint Surg Am.* 2022;104(4):379–89.
6. Blay JY, Honoré C, Stoeckle E, Meeus P, Jafari M, Gouin F, et al. Surgery in reference centers improves survival of sarcoma patients: a nationwide study. *Ann Oncol.* 2019;30(7):1143–53.
7. Brennan MF, Antonescu CR, Moraco N, Singer S. Lessons learned from the study of 10,000 patients with soft tissue sarcoma. *Ann Surg.* 2014;260(3):416–21.
8. Frei A, Scaglioni M, Giovanoli P, Breitenstein S, Heesen P, Fuchs B, et al. Definition of the surgical case complexity in the treatment of soft tissue tumors of the extremities and trunk. *Cancer.* 2022;14(6):1559.
9. Gronchi A, Lo Vullo S, Colombo C, Collini P, Stacchiotti S, Mariani L, et al. Extremity soft tissue sarcoma in a series of patients treated at a single institution: local control directly impacts survival. *Ann Surg.* 2010;251(3):506–11.
10. Sambri A, Caldari E, Montanari A, Fiore M, Cevolani L, Ponti F, et al. Vascular proximity increases the risk of local recurrence in soft-tissue sarcomas of the thigh—a retrospective MRI study. *Cancer.* 2021;13(24):6325.
11. Gerrand CH, Wunder JS, Kandel RA, O’Sullivan B, Catton CN, Bell RS, et al. The influence of anatomic location on functional outcome in lower-extremity soft-tissue sarcoma. *Ann Surg Oncol.* 2004;11(5):476–82.
12. Pritsch T, Bickels J, Winberg T, Malawer MM. Popliteal sarcomas: presentation, prognosis, and limb salvage. *Clin Orthop Relat Res.* 2007;455:225–33.
13. Gronchi A, Miah AB, Dei Tos AP, Abecassis N, Bajpai J, Bauer S, et al. Soft tissue and visceral sarcomas: ESMO-EURACAN-GENTURIS clinical practice guidelines for diagnosis, treatment and follow-up(☆). *Ann Oncol.* 2021;32(11):1348–65.
14. Wang D, Zhang Q, Eisenberg BL, Kane JM, Li XA, Lucas D, et al. Significant reduction of late toxicities in patients with extremity sarcoma treated with image-guided radiation therapy to a reduced target volume: results of radiation therapy oncology group RTOG-0630 trial. *J Clin Oncol.* 2015;33(20):2231–8.
15. Gilcrease-Garcia BM, Deshmukh SD, Parsons MS. Anatomy, imaging, and pathologic conditions of the brachial plexus. *Radiographics.* 2020;40(6):1686–714.
16. Tzeng CW, Smith JK, Heslin MJ. Soft tissue sarcoma: preoperative and postoperative imaging for staging. *Surg Oncol Clin N Am.* 2007;16(2):389–402.
17. Verga L, Brach del Prever EM, Linari A, Robiati S, de Marchi A, Martorano D, et al. Accuracy and role of contrast-enhanced CT in diagnosis and surgical planning in 88 soft tissue tumours of extremities. *Eur Radiol.* 2016;26(7):2400–8.
18. Kaiser D, Hoch A, Kriechling P, Graf DN, Waibel FWA, Gerber C, et al. The influence of different patient positions on the preoperative 3D planning for surgical resection of soft tissue sarcoma in the lower limb—a cadaver pilot study. *Surg Oncol.* 2020;35:478–83.
19. Piccinelli M. Multimodality image fusion, moving forward. *J Nucl Cardiol.* 2020;27(3):973–5.
20. Yu Z, Zhang W, Fang X, Tu C, Duan H. Pelvic reconstruction with a novel three-dimensional-printed, multimodality imaging based Endoprosthesis following Enneking type I + IV resection. *Front Oncol.* 2021;11:629582.
21. Fang X, Yu Z, Xiong Y, Yuan F, Liu H, Wu F, et al. Improved virtual surgical planning with 3D- multimodality image for malignant giant pelvic tumors. *Cancer Manag Res.* 2018;10:6769–77.
22. Grajales D, Kadoury S, Shams R, Barkati M, Delouya G, Béliveau-Nadeau D, et al. Performance of an integrated multimodality image guidance and dose-planning system supporting tumor-targeted HDR brachytherapy for prostate cancer. *Radiother Oncol.* 2021;166:154–61.
23. Nowell M, Rodionov R, Zombori G, Sparks R, Winston G, Kinghorn J, et al. Utility of 3D multimodality imaging in the implantation of intracranial electrodes in epilepsy. *Epilepsia.* 2015;56(3):403–13.
24. Network NCC. Soft tissue sarcoma. Version 2.2018. National Comprehensive Cancer Network; 2018.
25. Amin MB, Edge SB, Greene FL, et al, eds. *AJCC Cancer Staging Manual.* 8th ed. New York: Springer; 2017.
26. Fedorov A, Beichel R, Kalpathy-Cramer J, Finet J, Fillion-Robin JC, Pujol S, et al. 3D slicer as an image computing platform for the quantitative imaging network. *Magn Reson Imaging.* 2012;30(9):1323–41.
27. Trojani M, Contesso G, Coindre JM, Rouesse J, Bui NB, de Mascarel A, et al. Soft-tissue sarcomas of adults; study of pathological prognostic variables and definition of a histopathological grading system. *Int J Cancer.* 1984;33(1):37–42.
28. Gundle KR, Kafchinski L, Gupta S, Griffin AM, Dickson BC, Chung PW, et al. Analysis of margin classification systems for assessing the risk of local recurrence after soft tissue sarcoma resection. *J Clin Oncol.* 2018;36(7):704–9.
29. Enneking WF, Dunham W, Gebhardt MC, et al. A system for the functional evaluation of reconstructive procedures after surgical treatment of tumors of the musculoskeletal system. *Clin Orthop Relat Res.* 1993;286:241–6.
30. Huang ZY, Huang Q, Wang LY, Lei YT, Xu H, Shen B, et al. Normal trajectory of Interleukin-6 and C-reactive protein in the perioperative period of total knee arthroplasty under an enhanced recovery after surgery scenario. *BMC Musculoskelet Disord.* 2020;21(1):264.
31. Watt DG, McSorley ST, Horgan PG, McMillan DC. Enhanced recovery after surgery: which components, if any, impact on the systemic inflammatory response following colorectal surgery? A systematic review. *Medicine.* 2015;94(36):e1286–6.
32. Hagi T, Nakamura T, Nagano A, Koike H, Yamada K, Aiba H, et al. Clinical outcome in patients who underwent amputation due to extremity soft tissue sarcoma: Tokai Musculoskeletal Oncology Consortium study. *Jpn J Clin Oncol.* 2022;52(2):157–62.
33. Iezzoni LI, Daley J, Heeren T, Foley SM, Fisher ES, Duncan C II, et al. Identifying complications of care using administrative data. *Med Care.* 1994;32(7):700–15.
34. Shirk JD, Thiel DD, Wallen EM, Linehan JM, White WM, Badani KK, et al. Effect of 3-dimensional virtual reality models for surgical planning of robotic-assisted partial nephrectomy on surgical outcomes: a randomized clinical trial. *JAMA Netw Open.* 2019;2(9):e1911598.